Zygote **22** (May), pp. 218–228. © Cambridge University Press 2013
doi:10.1017/S0967199413000051 First Published Online 27 March 2013

Biphasic assembly of the contractile apparatus during the first two cell division cycles in zebrafish embryos

Sarah E. Webb[2], *Cécile Goulet*[2], *Ching Man Chan*[2], *Michael Y. F. Yuen*[2] *and Andrew L. Miller*[1,3]
Division of Life Science and State Key Laboratory of Molecular Neuroscience, The Hong Kong University of Science & Technology, Clear Water Bay, Kowloon, Hong Kong, People's Republic of China; and Marine Biological Laboratory, Woods Hole, Massachusetts 02543, USA

Date submitted: 16.03.2012. Date accepted: 30.05.2012

Summary

The large and optically clear embryos of the zebrafish provide an excellent model system in which to study the dynamic assembly of the essential contractile band components, actin and myosin, via double fluorescent labelling in combination with confocal microscopy. We report the rapid appearance (i.e. within <2 min) of a restricted arc of F-actin patches along the prospective furrow plane in a central, apical region of the blastodisc cortex. These patches then fused with each other end-to-end forming multiple actin cables, which were subsequently bundled together forming an F-actin band. During this initial assembly phase, the F-actin-based structure did not elongate laterally, but was still restricted to an arc extending ~15° either side of the blastodisc apex. This initial assembly phase was then followed by an extension phase, where additional F-actin patches were added to each end of the original arc, thus extending it out to the edges of the blastodisc. The dynamics of phosphorylated myosin light chain 2 (MLC2) recruitment to this F-actin scaffold also reflect the two-phase nature of the contractile apparatus assembly. MLC2 was not associated with the initial F-actin arc, but MLC2 clusters were recruited and assembled into the extending ends of the band. We propose that the MLC2-free central region of the contractile apparatus acts to position and then extend the cleavage furrow in the correct plane, while the actomyosin ends alone generate the force required for furrow ingression. This biphasic assembly strategy may be required to successfully divide the early cells of large embryos.

Keywords: Actin, Biphasic, Meroblastic cell division, Myosin light chain 2, Zebrafish

Introduction

In small diameter (i.e. ~50–100 μm) holoblastically dividing eggs, such as those of echinoderms, the first cleavage furrow appears almost instantaneously around the entire circumference of the egg cell (Rappaport, 1996). This situation suggests that in these relatively small animal cells the contractile band (or ring) that subsequently mediates furrow ingression, is also positioned and assembled in a near-simultaneous manner in the cleavage plane around the circumference of the egg cell cortex (Schroeder, 1975; Mabuchi, 1994). However, in the case of large diameter (i.e. ~500–1500 μm) eggs that divide in either a holoblastic or meroblastic manner, such as those of amphibians and teleosts, respectively, the first cleavage furrow initially appears as a restricted arc on the egg surface. It then begins to propagate in a linear manner from each end of the arc. In the case of medaka (*Oryzias latipes)*, mummichog (*Fundulus heteroclitus*) and zebrafish (*Danio rerio)* embryos, the furrow propagates to the meroblastic limits of its extension (Lentz & Trinkaus, 1967; Kimmel & Law, 1985; Fluck *et al.*, 1991). Alternatively, in amphibian embryos such as those of the African clawed frog (*Xenopus laevis*) or Alpine newt (*Triturus alpestris),* which undergo holoblastic division, the leading ends

[1]All correspondence to: Andrew L. Miller. Division of Life Science, The Hong Kong University of Science & Technology, Clear Water Bay, Kowloon, Hong Kong, People's Republic of China. Tel: +1 852 2358 8631. Fax: +1 852 2358 1559. e-mail: almiller@ust.hk
[2]Division of Life Science and State Key Laboratory of Molecular Neuroscience, The Hong Kong University of Science & Technology, Clear Water Bay, Kowloon, Hong Kong, People's Republic of China.
[3]Marine Biological Laboratory, Woods Hole, Massachusetts 02543, USA.

of the furrow continue to propagate through the egg cortex until they meet in the vicinity of the vegetal pole (Selman & Perry, 1970; Denis-Donini *et al.*, 1976; Takayama *et al.*, 2002). In the case of large eggs that display this biphasic furrowing strategy, it suggests that there might also be two phases to the assembly and propagation of the underlying contractile band. The first phase results in the near-instantaneous positioning of a restricted contractile arc in the egg cortex, which is aligned with the future cleavage plane (i.e., in a manner similar to the complete circumferential appearance of the contractile ring seen in smaller eggs). This is then followed by a second phase of contractile band assembly as it propagates through the cortex, further defining the division plane of the large egg cell. Such a process has been reported during the early holoblastic cleavages of *Xenopus* embryos. Noguchi & Mabuchi (2001) visualized the reorganization of the cortical actin cytoskeleton as well as the dynamics of myosin II distribution at the growing ends of the cleavage furrow of *Xenopus* embryos following the positioning step of the initial furrowing arc.

The furrowing strategy in large meroblastically dividing teleost eggs also appears to be more complex than that in small holoblastically dividing eggs. Stone *et al.* (1993) reported that during the first few cell divisions in medaka eggs, the first sign of cytokinesis following the metaphase–anaphase transition is the formation of an 'internal' furrow that appears at the inner surface between the blastodisc and the underlying yolk vacuole, rather than the formation of a surface indentation on the external surface of the blastodisc. This observation supported an earlier report from medaka by Kamito (1928), and from the dividing eggs of four species of pelagic fish: two species of wrasse and two of flounder (*Ctenolabrus* sp. and *Tautoga* sp., as well as *Pseudorhombus melanogaster* and *Ps. oblongus*, respectively; Agassiz & Whitman, 1884). In medaka, the external furrow appears ~7 min after the internal furrow, and does so in the same plane. The external furrow appears initially as a shallow arc at the apex of the blastodisc, the ends of which then propagate outward toward the margin of the blastodisc while deepening at the same time (Fluck *et al.*, 1991). Following this propagation and deepening process, the separated daughter cells then 'zip-up', undergoing a process of cell apposition (Fluck *et al.*, 1991; Webb *et al.*, 2011). The relationship/interaction between the growing ends of the external and the internal furrows in medaka eggs is as yet unclear, but it has been reported that as the external furrow ingresses, the internal furrow regresses (Stone *et al.*, 1993).

The appearance of an internal furrow has not been reported during the early divisions of the zebrafish blastodisc, as it has in the medaka. The cytoplasm of the medaka egg, however, unlike that of the zebrafish, is bounded by two membranes: the plasma membrane at its outer (external) surface, which separates the cytoplasm from the perivitelline space; and a yolk membrane at its inner (internal) surface, which separates the cytoplasm from the large, central yolk cell (Kamito, 1928; Fluck *et al.*, 1991). In zebrafish, there is, therefore, no inner membrane to ingress. However, the floor of the blastodisc in zebrafish, where the cytoplasm comes directly into contact with the underlying yolk platelets (Kimmel & Law, 1985), can be seen to rise-up to meet the ingressing cleavage furrow during the first few cell division cycles (Webb *et al.*, 1997; Fuentes & Fernández, 2010). This event suggests that in zebrafish there still is some as yet unexplained interaction between the ingressing plasma membrane and the floor of the blastodisc. It has been reported from zebrafish that during early divisions, when the ingressing furrow reaches the blastodisc floor, it changes to a horizontal orientation to partially undercut the blastodisc (Kimmel *et al.*, 1995). This partial undercutting, however, still leaves the early zebrafish blastomeres only partially separated from the underlying yolk platelets, thus, they remain connected via the underlying yolk cell. During the early meroblastic cleavages of the sea bass (*Serranus atarius* syn. *Centropristis atarius*) the early ingressing furrows were reported to cut deeply into the blastodisc but they do not, however, extend all the way through to the underlying yolk (Wilson, 1889). Thus, the daughter cells resulting from early cell divisions remain connected together by a thin layer of cytoplasm that was termed the 'central periblast'. With regards to the appearance of a cleavage furrow on the outer, external surface of the zebrafish blastodisc, it has been proposed that there may be up to four sequential phases with respect to early divisions. These are: A furrow positioning phase; followed by a furrow propagation phase (with little furrow deepening); followed by a furrow deepening phase; then finally once the daughter cells have been separated, a furrow zipping or apposition phase (Lee *et al.*, 2004, 2006; Li *et al.*, 2008).

With respect to the positioning and assembly of the contractile band in the blastodisc cortex of zebrafish, F-actin has been reported to accumulate near the centre of the blastodisc, coincident with the initial phase of furrow formation. Such an accumulation of F-actin is absent or abnormal in mutants affecting the initiation of cytokinesis (Kishimoto *et al.*, 2004). This initial increase in F-actin at the animal pole then results in the formation of two distinct F-actin-based structures. The first is an array of long parallel F-actin cables, which are aligned along the plane of the cleavage furrow then subsequently bundle together to form the contractile band. The second has been described as a pair of

peri-cleavage F-actin enrichments (PAEs), which are lamella-like structures that form on either side of the contractile band and contribute to the addition of new membrane and the eventual apposition of the daughter cells (Urven *et al.*, 2006; Li *et al.*, 2008). The dynamic F-actin remodelling associated with the formation of both the contractile band and the PAEs during zebrafish cytokinesis has been reported to be Ca^{2+} dependent (Chang & Meng, 1995; Webb *et al.*, 1997; Li *et al.*, 2008), although the precise mechanism(s) by which localized elevations in free Ca^{2+} mediate their effect, remain elusive. Our understanding of the recruitment and specific contribution of non-muscle myosin II to the forming contractile band and the generation of force during the meroblastic division in zebrafish embryos is somewhat limited. It has been reported, however, that exposure to inhibitors of non-muscle myosin function (e.g. blebbistatin and ML7) do not affect furrow ingression during early cleavage cycles, but do interfere with the recruitment of F-actin to the PAEs and subsequent furrow maturation (Urven *et al.*, 2006).

In this new study, we report the rapid appearance at the zebrafish blastodisc apex of oriented, elongated patches of F-actin that assemble in an end-to-end manner to form F-actin cables. These cables then rapidly bundle together to form an initial F-actin arc. The orientation of the arc defines the plane of the subsequent cell division. We propose that the formation of this arc is the first step in a biphasic process that eventually leads to the propagation of the contractile band to its meroblastic limits at the edge of the blastodisc. The second phase of this process is the subsequent extension of the initial arc via the addition of F-actin patches, followed by F-actin cable bundling, at the growing ends of the arc. Furthermore, we describe the recruitment of phosphorylated myosin light chain 2 (MLC2; one of the light chains of myosin II) specifically during the second phase of contractile band assembly, where it co-localizes only with the newly added F-actin-based scaffold that extends out from the ends of the initial arc. The pattern of myosin recruitment thus supports our biphasic model of contractile apparatus assembly. We also report the coincidental appearance of highly localized calmodulin domains associated with the formation of the initial arc and the PAEs. Calmodulin has been previously reported to be localized in the cleavage furrow during cytokinesis in HeLa cells and in the ciliated protozoan, *Tetrahymena thermophila*, and when calmodulin expression or function was inhibited, cytokinesis was blocked (Gonda *et al.*, 1999; Li *et al.*, 1999). It was suggested that in small mammalian cells, the cleavage furrow might be positioned by a localized increase in calmodulin rather than by Ca^{2+} (Li *et al.*, 1999). Our data suggest that in the large dividing cells of embryos, calmodulin also plays a role in cytokinesis perhaps as a significant downstream target of the cytokinetic Ca^{2+} transients reported previously (Chang & Meng, 1995; Webb *et al.*, 1997).

These observations have led us to propose that during the early meroblastic divisions of the zebrafish blastodisc, the middle, MLC2-free portion of the contractile band does not generate any significant contractile force. However, the actomyosin-rich regions located at the lateral ends of the contractile band represent the main sites of force generation required for cleavage. We liken this process to a wire cheese-cutter in which force is generated at the ends of the wire. Thus, the role of the central, MLC2-free portion of the contractile band is to help position the furrow in the correct orientation; provide a scaffold from which the contractile portion of the band can assemble and extend from; and provide a structural means by which the force generated by the contractile ends of the band can mediate the ingression of the plasma membrane and the subsequent separation of the daughter cells.

Materials and methods

Embryo collection

The AB strain of zebrafish (obtained from the Zebrafish International Resource Centre; University of Oregon, Eugene, OR, USA) were maintained on a 14 h light/10 h dark cycle to stimulate spawning (Westerfield, 1994). Fertilized eggs were collected and embryos were maintained in 30% Danieau's solution (17.4 mM NaCl, 0.21 mM KCl, 0.18 mM $Ca(NO_3)_2$, 0.12 mM $MgSO_4.7H_2O$, 1.5 mM HEPES, pH 7.2) at ~28.5°C throughout development and during all experiments, as described by Webb *et al*. (1997).

F-actin and myosin labelling

Rhodamine-tagged phalloidin (Sigma-Aldrich Co., St Louis, MO, USA) was used to label F-actin, and the rabbit polyclonal phospho-myosin light chain 2 (Ser 19) antibody (Cell Signaling Technology Inc., Beverly, MA, USA) was used to label endogenous levels of myosin light chain 2 (MLC2) when phosphorylated at serine 19, in the forming contractile apparatus of zebrafish embryos during the first and second cell division cycles.

Embryos were dechorionated by treatment with pronase (Sigma-Aldrich Co.) as described previously (Leung *et al.*, 1998) and then fixed at various times during the first cell division cycle with 4% paraformaldehyde in phosphate-buffered saline (PBS pH 7.3; Westerfield, 1994) overnight at 4°C, after which they were washed thoroughly with PBS. They were

https://doi.org/10.1017/S0967199413000051 Published online by Cambridge University Press

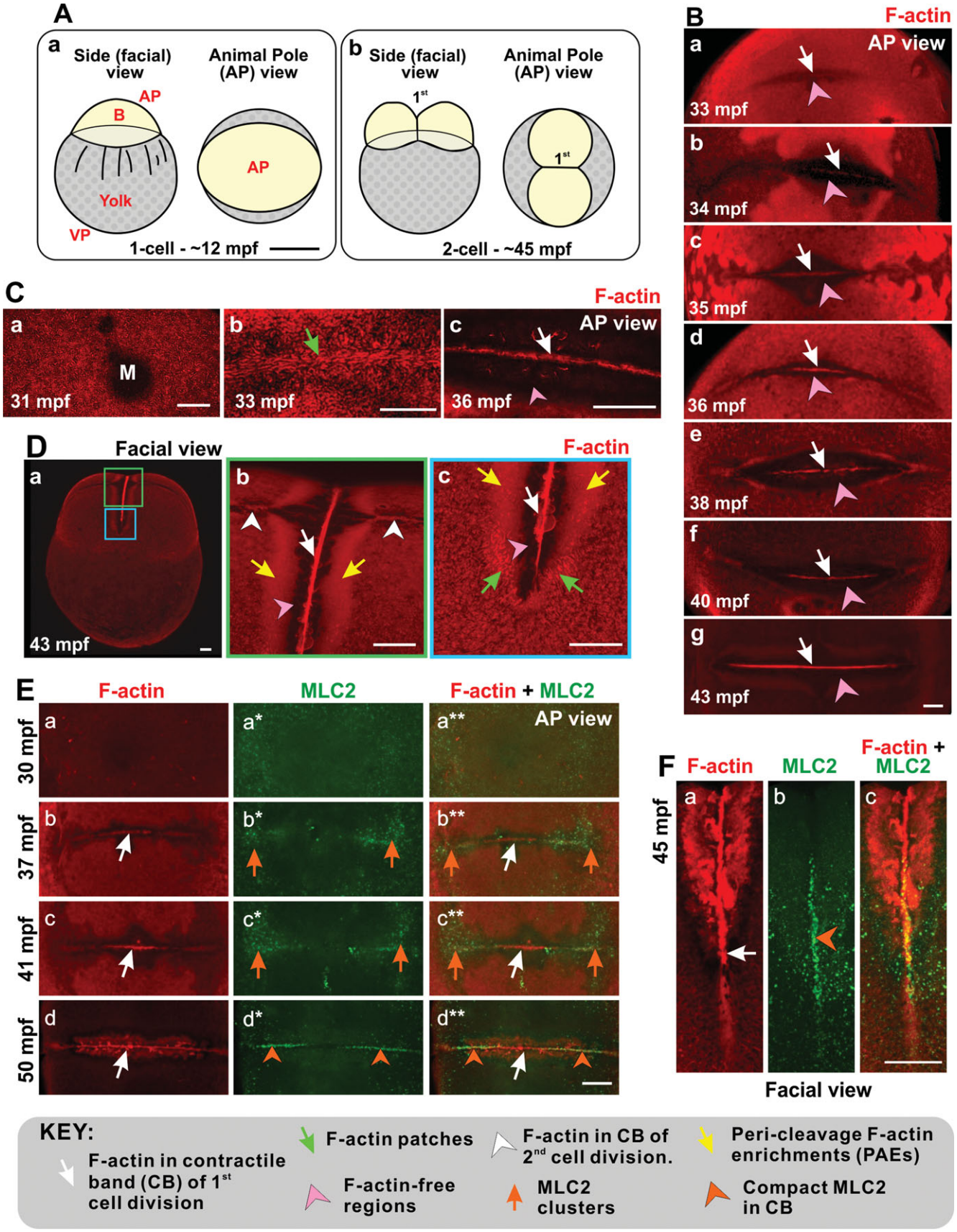

Figure 1 Assembly of the contractile band during the first cell division cycle. (*A*) Schematic representation of a zebrafish embryo at the 1-cell stage (*Aa*) and 2-cell stage (*Ab*). AP and VP are animal and vegetal pole, respectively; B is blastodisc

https://doi.org/10.1017/S0967199413000051 Published online by Cambridge University Press

washed briefly with PBS that contained 0.1% Tween-20 (PBS-T0.1) and then incubated with PBS that contained 0.5% Tween-20 (PBS-T0.5) for 1 h, after which they were incubated with blocking buffer (PBS-T0.5 that contained 10% goat serum) at room temperature for 5 h.

In some experiments, embryos were then incubated immediately with rhodamine-tagged phalloidin (Sigma-Aldrich Co.) at 1:100 in blocking buffer and incubated for 1 h at room temperature in the dark, after which they were washed with PBS-T0.5.

In another series of experiments, embryos were incubated following the blocking step with the phospho-myosin light chain 2 (Ser19) antibody (at a dilution of 1:10) overnight at 4°C in the dark. They were then washed extensively with PBS-T0.5 and incubated with a fluorescein isothiocyanate (FITC)-conjugated goat anti-rabbit IgG (Zymed Laboratories, Invitrogen, Carlsbad, CA, USA) diluted 1:100 in blocking buffer for 5 h at room temperature, after which they were washed extensively again with PBS-T0.5 in the dark. The embryos were then labelled with rhodamine-tagged phalloidin at 1:100 in blocking buffer and incubated for 1 h at room temperature in the dark, after which they were washed with PBS-T0.5 prior to visualization via confocal microscopy.

Calmodulin labelling

Embryos were fixed at various times between the one- and four-cell stage and then a mouse monoclonal anti-calmodulin IgG_1 (Upstate Inc., Lake Placid, NY, USA) was used to label calmodulin in the cleavage furrow. Embryos were fixed as described above. They were then washed thoroughly with PBS, rinsed briefly with PBS-T0.1 and incubated with PBS-T0.1 that contained 1% dimethyl sulphoxide (DMSO) (PBS-TD) at room temperature for 1 h. The embryos were then incubated with blocking buffer (10% goat serum (Invitrogen Corp.) in PBS-TD) for 2 h, after which they were incubated with the anti-calmodulin IgG_1 at a 1:50 dilution in blocking buffer overnight at 4°C. The embryos were then washed extensively with 1% goat serum in PBS-TD before being incubated with a FITC-conjugated goat anti-mouse IgG (Sigma-Aldrich Co.) at a 1:50 dilution in blocking buffer overnight at 4°C in the dark. The embryos were finally washed with PBS prior to visualization via confocal microscopy.

Confocal microscopy

Embryos were examined with a Nikon C1 laser scanning confocal system mounted on an Eclipse 90i microscope using Nikon Fluor ×20/0.5NA and ×40/0.8NA water-dipping objective lenses. FITC fluorescence was captured using a 488 nm excitation wavelength and a 515/530 nm emission filter, while rhodamine fluorescence was captured using a 543 nm excitation wavelength and 570 nm (long pass) emission filter. Embryos were held in imaging chambers (Webb *et al.*, 1997) and oriented such that the blastodisc could be observed from an animal pole or facial view. Images were exported to Corel Draw X5 for subsequent figure preparation.

Results and Discussion

Distribution of F-actin and MLC2 during assembly of the contractile band.

Embryos were fixed at various times during the first cell division cycle (i.e., from the one- to two-cell stage; Fig. 1*A*) and then phosphorylated myosin light chain 2 (MLC2) and/or F-actin was labelled and the region of the blastodisc encompassing the cleavage furrow was visualized from an animal pole or side (facial) view by confocal microscopy.

In order to determine the localization of F-actin in the forming contractile band during the first cell division, embryos were fixed at one minute intervals between ∼33 min post-fertilization (mpf) and ∼36 mpf and then at ∼38 mpf, ∼40 mpf and ∼43 mpf, after which they were labelled with rhodamine-tagged phalloidin (Fig. 1*B*). At ∼33 mpf, a distinct arc of aligned F-actin patches was observed in the central apical region of the blastodisc cortex (white arrow in Fig. 1*Ba*). This initial F-actin-based arc extended ∼15° on either side of the apex of the blastodisc, and the orientation of the arc determined the future

and 1st refers to the plane of cleavage of the first cell division cycle. (*B*) Animal pole views to show the distribution of F-actin in the assembling contractile band (CB) at various times from ∼33 min post-fertilization (mpf) to ∼43 mpf (*a*–*g*). (*C*) Higher magnification animal pole views that were acquired prior to (i.e., at ∼31 mpf, (*Ca*)) and during (i.e., at ∼33 mpf (*Cb*) and ∼36 mpf (*Cc*)) the formation of the CB. M, micropyle. (*D*) Oblique-facial views of the CB at ∼43 mpf. The regions bounded by the green and blue squares in panel (*Da*) are shown at higher magnification in panels (*Db*) and (*Dc*), respectively. (*E*) Animal pole views to show the localization of F-actin and phosphorylated-myosin light chain 2 (Ser19; MLC2) in the cleavage furrow from ∼30 mpf to ∼50 mpf. (*F*) Facial view of the CB to show the localization of F-actin and MLC2 at ∼45 mpf. Each image is a projected stack of confocal optical sections. The key describes the arrows and arrowheads used in each panel. Scale bars are (*A*) 250 μm; (*B*, *D*, *E*, *F*) 50 μm and (*C*) 20 μm.

https://doi.org/10.1017/S0967199413000051 Published online by Cambridge University Press

cleavage plane. We suggest that the rapid positioning and assembly of this cortical F-actin arc (i.e., within <2 min) represents the first phase of a biphasic contractile apparatus assembly process. The recruitment of F-actin to the initial arc leaves distinct F-actin-free regions (pink arrowhead in Fig. 1*Ba*) in the cortex on either side of the forming F-actin arc. This finding suggests that some of the F-actin that forms the arc was recruited from these regions. These clear regions were apparent at all the time points observed and their lateral extremities extended in conjunction with the subsequent extension of the contractile band. Between ~34 mpf and ~36 mpf (Fig. 1*Bb–Bd*) the F-actin arc became more distinct without appearing to extend laterally, and then between ~38 mpf and ~43 mpf (Fig. 1*Be–Bg*) it started to extend beyond the initial lateral extremities along the remainder of the furrow plane toward the edge of the blastodisc. Thus, we suggest that the contractile apparatus develops in a biphasic manner consisting of an initial rapid positioning and assembly phase, followed by a slower extension phase of the band to its meroblastic limits at the edge of the blastodisc.

The initial assembly phase of the F-actin arc was also observed at higher magnification (Fig. 1*C*). Prior to assembly of the arc, clusters of F-actin appeared to be evenly distributed in the blastodisc cortex around the actin-free micropyle ('M' in Fig. 1*Ca*). During the early stages of arc assembly, the F-actin clusters rapidly (i.e., within <2 min) reorganized into distinct elongated F-actin patches that were oriented along the plane of the first cell division (green arrow; Fig. 1*Cb*). The F-actin patches then fused together end-to-end, to form multiple F-actin cables. The individual actin cables were then bundled together into a compact arc array that defined the first cleavage plane of the blastodisc (white arrow; Fig. 1*Cc*). The F-actin-free clear zone was just beginning to form and was therefore not very obvious when the F-actin clusters were reorganizing into F-actin patches (Fig. 1*Cb*). However, this clear zone was more apparent when the F-actin cables were assembling and being bundled into a more compact arc (pink arrowhead in Fig. 1*Cc*). This supports our suggestion that the clear zones form in part as a result of F-actin being recruited to the contractile apparatus.

The second phase of contractile band extension is also shown at higher magnification from a facial view (Fig. 1*D*, embryo fixed at 43 mpf). The regions bounded by the green and blue squares in Fig. 1Da are shown at higher magnification in Fig. 1*Db* and 1*Dc*, respectively. At the animal pole (Fig. 1*Db*), the contractile band of the first cell division (white arrow) as well as a pair of distinct remodelled cortical actin domains, called pericleavage F-actin enrichments (PAEs; yellow arrows; Urven *et al.*, 2006; Li *et al.*, 2008) are shown. The F-actin-free regions between the contractile band and PAEs are also visible (pink arrowhead), as are the assembling contractile bands of the second cell division cycle (white arrowheads).

An accumulation of elongated F-actin patches (green arrows; Fig. 1*Dc*) can also be seen around the lateral extremities at the growing end of the extending contractile band, suggesting that these growing ends are actively extending towards the edges of the blastodisc via recruitment of the F-actin patches. Away from the growing ends, both the F-actin-free zones and the F-actin-based PAEs can be clearly seen (pink arrowhead and yellow arrows, respectively).

In another series of experiments, in addition to labelling F-actin, a phospho-myosin light chain 2 antibody was used to label myosin light chain 2 (MLC2) via indirect immunohistochemistry (Fig. 1*E, F*). During the assembly of the initial F-actin arc, MLC2 was not recruited along with F-actin patches (white arrow in Fig. 1*Eb–Ed*, *Eb**–Ed***) at the apex of the blastodisc. It did, however, begin to localize in clusters toward the furrow plane during the band extension phase (orange arrows; Fig. 1*Eb**,*Ec**,*Eb***,*Ec***). As the extending F-actin band became more compact, the localization of MLC2 clusters also became more compact (orange arrowheads; Fig. 1*Ed**) until they became co-localized with the F-actin component in the extending contractile band (orange arrowheads; Fig. 1*Ed***) as the latter reached the edge of the blastodisc. The clusters and co-localization of MLC2 with F-actin in the contractile band can also be observed from a facial view (Fig. 1*F*).

Our new data suggest that the recruitment of MLC2 clusters to the furrow plane appears to extend beyond (by ~30 μm) the highly compact F-actin arc, but not the more diffuse F-actin patch recruitment zone which extends beyond the MLC2 clustering by ~50 μm (compare Fig. 1*Fa* with 1*Fb*, and see overlay in Fig. 1*Fc*). This situation would appear to be somewhat similar to what has been reported during the assembly and extension of the contractile apparatus through the cortex of *Xenopus* eggs during the early cleavage cycles. Noguchi & Mabuchi (2001) reported that the first elements to appear at the extending ends of the contractile apparatus were accumulations of myosin II (which they termed 'myosin spots') that took the form of clusters of short myosin mini-filaments. This action was then followed by the accumulation of F-actin into F-actin patches, thus suggesting that actin polymerization takes place after the assembly of myosin at the same location. They also reported, however, the presence of what they described as 'dimly stained F-actin patches' that could be seen before the compact accumulation of F-actin at the growing end of the contractile apparatus. They thus proposed that it was possible that a precursor of the F-actin patches may be simultaneously formed

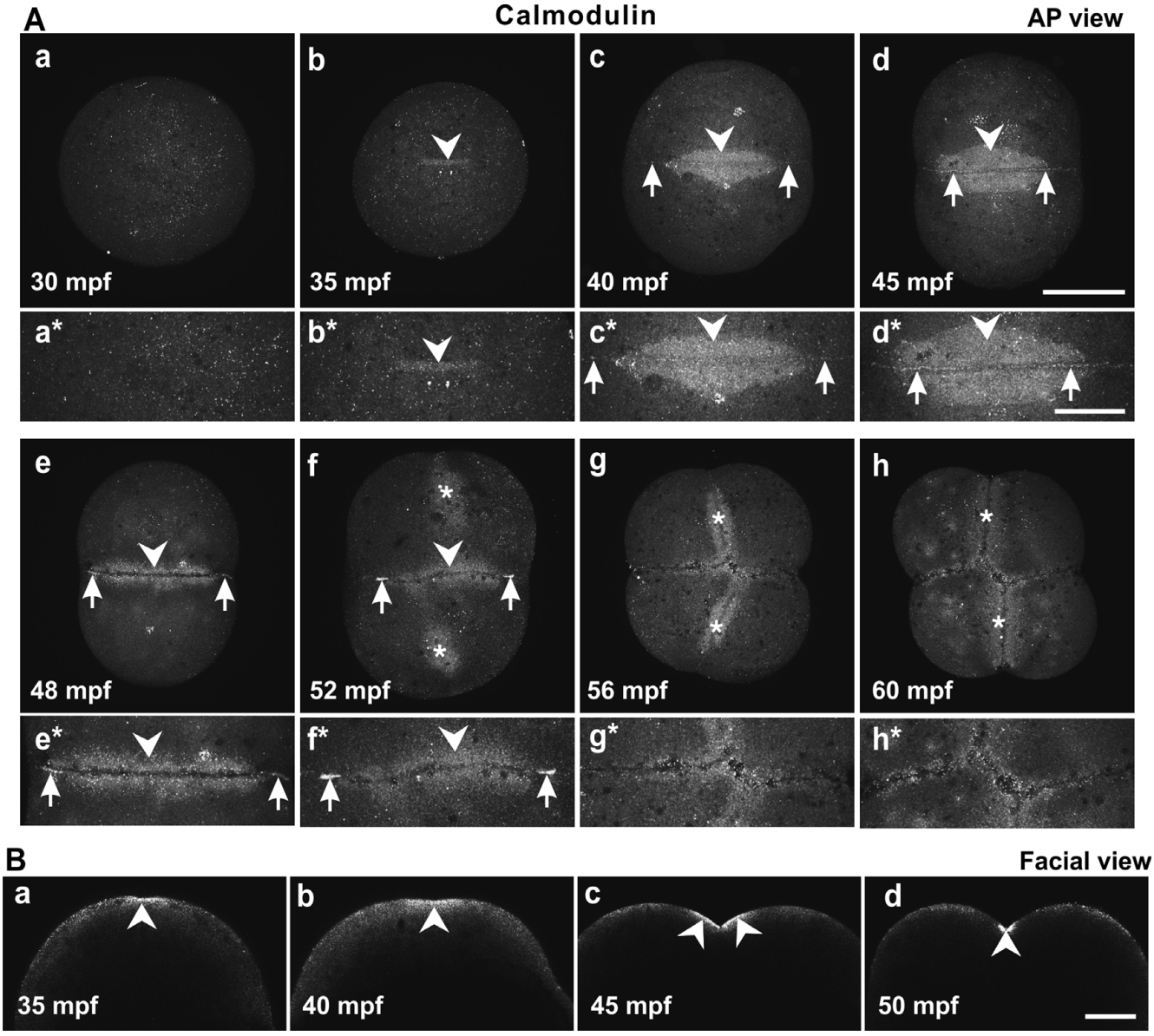

Figure 2 Localization of calmodulin in the cleavage furrows during the first and second cell division cycles. (*A*, *B*) Representative embryos ($n = 4$) that were fixed at the time points indicated (bottom left corner of images *Aa–Ah* and *Ba–Bd*) and then calmodulin was labelled via indirect immunohistochemistry. These are (*A*) stacks of confocal sections taken through the animal pole that were projected as single images and (*B*) single optical sections of the blastodisc from a facial view. Panels *a**–*h** in (*A*) are high magnification views of the forming cleavage furrow taken from panels *a–h*, respectively. Arrowheads and asterisks indicate localization of calmodulin in the first and second cleavage furrows, respectively while arrows indicate the expression of calmodulin in the contractile band. Scale bars are 200 μm (*Aa –Ah*) and 100 μm (*Aa**–*Ah**, *B*).

along with the myosin spots. As the F-actin patches elongate and fuse together to form cables, followed by the subsequent bundling of the F-actin cables to form a compact arc, the organization of myosin in the spots was also reported to change in a manner parallel to that of the F-actin, i.e., the myosin spots were also seen to elongate and fuse with one another (Noguchi & Mabuchi, 2001). This observation is supported by reports from fission yeast where the organization of myosin into the contractile ring requires an interaction between F-actin and myosin (Naqvi *et al.*, 1999; Motegi *et al.*, 2000). It was suggested, therefore, that some form of F-actin-myosin interaction might be a common feature in the assembly and extension of the contractile apparatus in animal and fungal cells. Furthermore, it has been proposed that multiple redundant mechanisms serve to control myosin activity in order to make its recruitment to the contractile apparatus as robust as possible (Uehara *et al.*, 2010). It is likely that during cytokinesis, the

https://doi.org/10.1017/S0967199413000051 Published online by Cambridge University Press

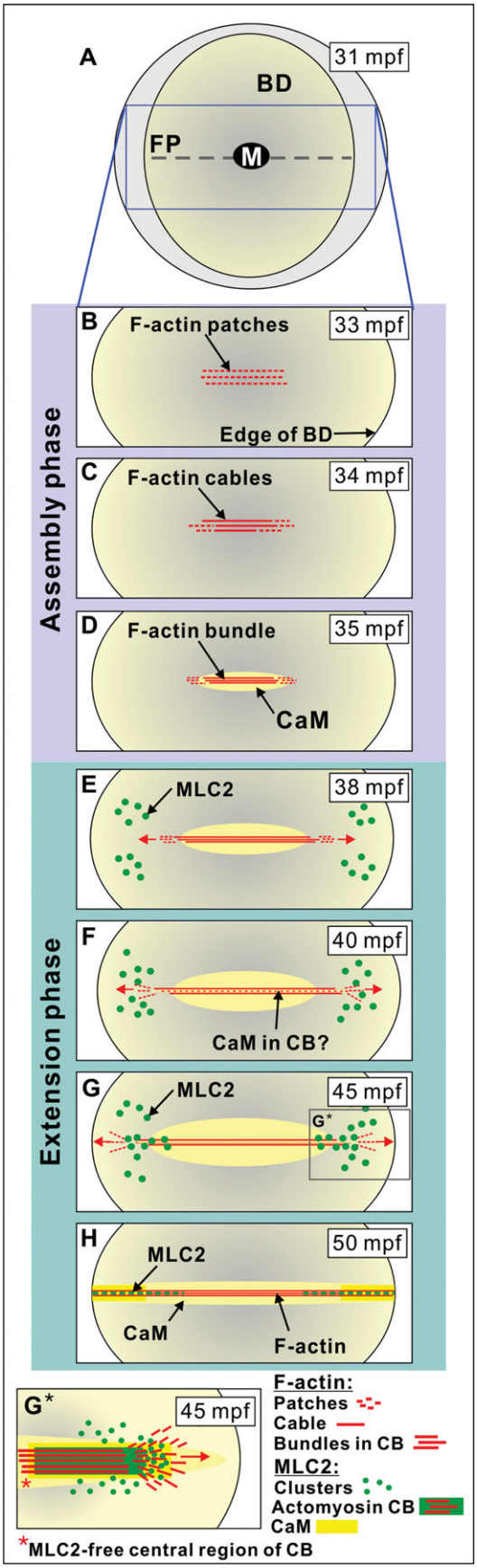

timing and degree to which each of these mechanisms contributes to the localization of myosin to the contractile apparatus varies between cell types. A key factor contributing to this variability is likely to be cell size. Thus, in small cells myosin may be recruited and spatially restricted to the equatorial cortex (Yumura *et al.*, 2008), whereas in large cells the localization domain may be around the extending end of the contractile apparatus (Noguchi & Mabuchi, 2001), as would appear to be the case in the zebrafish blastodisc (Fig. 1*E*, 1*F*).

Distribution of calmodulin in the cleavage furrow during the first two-cell division cycles

Embryos were fixed at various times during the first and second cell division cycles and then calmodulin was labelled via immunohistochemistry and the region of the blastodisc encompassing the cleavage furrow was visualized from an animal pole (Fig. 2*A*) or side (facial) view (Fig. 2*B*) by confocal microscopy. When looking at multiple optical sections that were projected as a single image from an animal pole view, no calmodulin labelling was detected in the blastodisc at ~30 mpf (Fig. 2*Aa*, *Aa**). The first sign of calmodulin labelling was observed at ~35 mpf when an arc of fluorescence appeared at the apex of the blastodisc (white arrowhead in Fig. 2*Ab*, *Ab**). At ~40 mpf the region of calmodulin labelling extended in both length and width across the blastodisc (white arrowhead in Fig. 2*Ac*, *Ac**). There was a distinct line of lower calmodulin labelling, which bisected the labelling on either side of the furrow, along the plane of the forming contractile band. We suggest that this pattern of labelling developed in conjunction with the propagation and initial deepening of the first cleavage furrow. In the next 5 min the region of calmodulin labelling did not extend any further in length but did increase in width, and within the central region of lower calmodulin labelling, a distinct line of more highly localized calmodulin labelling was now apparent extending along the base of the furrow (white arrows in Fig. 2*Ad*, *Ad**). We suggest that at this time point, cleavage furrow deepening was well underway. At ~48 mpf, the region of calmodulin labelling had extended in length again but the width had narrowed. In addition, the line of localized calmodulin labelling

Figure 3 Hypothetical model to illustrate a top view of our proposed biphasic dynamic assembly and extension of the actomyosin contractile band (CB) and associated localization of calmodulin during the first cell division cycle. BD, blastodisc edge; CaM, calmodulin; FP, prospective furrow plane; M, micropyle; MLC2, phosphorylated myosin light chain 2.

https://doi.org/10.1017/S0967199413000051 Published online by Cambridge University Press

was reduced at the middle of the furrow but was still obvious in the furrow at the edges of the blastodisc (white arrows in Fig. 2*Ae, Ae**). We suggest that this latter observation reflects our proposition that it is the lateral ends of the contractile apparatus that generate force and thus require the presence of calmodulin to regulate this process. We also suggest that the narrowing of the width of calmodulin labelling is due to the furrow just completing deepening and starting to undergo apposition. At ~52 mpf (Fig. 2*Af, Af**), calmodulin labelling in the cleavage furrow of the first cell division cycle was similar to that observed at ~48 mpf, and expression was also detected at the sites of the cleavage furrow of the second cell division cycle (white asterisks in Fig. 2*Af*). Over the next two time points (i.e. at ~56 mpf and ~60 mpf, Fig. 2*Ag, Ag*, Ah, Ah**), the level of labelling of calmodulin in the first cleavage furrow declined, while that in the second cleavage furrows initially became more prominent and then declined, following a similar pattern of labelling to that described for the first cell division cycle.

We also visualized the pattern of calmodulin labelling during the first cell division cycle with the blastodisc in a facial orientation (Fig. 2*B*). These four single optical sections acquired through the middle of the blastodisc show that the labelling of calmodulin remained in a cortical location during cytokinesis (Fig. 2*B*), that it was initially visible before an obvious furrow had started to form (which would be indicated by an indentation) at the apex of the blastodisc (Fig. 2*Ba*), and they confirm the dimensional changes in width during propagation (Fig. 2*Bb*), deepening (Fig. 2*Bc*) and apposition (Fig. 2*Bd*), observed in the animal pole view images shown in Fig. 2*A*.

It has been reported from HeLa cells that the distribution pattern of a GFP-calmodulin fusion protein is the same as endogenous calmodulin (Li *et al.*, 1999). In HeLa cells undergoing cytokinesis, GFP-calmodulin was seen to be translocated from a general distribution all around the cortex of the cell, to a specific sub-membrane location coincidental to that of the cleavage plane. In zebrafish, however, we did not observe a redistribution of endogenous calmodulin; rather we visualized the appearance of calmodulin at the cleavage plane suggesting the *de novo* synthesis of calmodulin at this specific location. The spatial and temporal nature of the calmodulin labelling closely matches the same parameters of the Ca^{2+} transients that have been reported during the first few cell division cycles in zebrafish (Chang & Meng, 1995; Webb *et al.*, 1997). This finding suggests that calmodulin might act as one of the downstream targets for these cytokinetic Ca^{2+} transients. Furthermore, it has been proposed that one of the targets of Ca^{2+}-activated calmodulin might be myosin light chain kinase (MLCK), resulting in the generation of contractile force by the actomyosin-based contractile apparatus (Satterwhite *et al.*, 1992; Matsumura, 2005; Urven *et al.*, 2006). Previous reports, which indicate that the Ca^{2+} waves mediating the deepening of the cleavage furrow in zebrafish linger at the lateral extremities of the contractile band (Webb *et al.*, 1997; Lee *et al.*, 2003) support our new proposition that the lateral ends of the contractile band, where both actin and MLC2, as well as calmodulin, were shown to co-localize, are the major regions of force generation during cleavage furrow ingression.

Conclusions

During the initial assembly phase, the contractile band rapidly appears in the blastodisc cortex as a discontinuous assembly of oriented F-actin patches. These patches then fuse together to form numerous actin cables, and the cables are subsequently bundled into a compact F-actin-based arc. The lateral extensions of this initial structure appear to be limited to an arc extending ~15° on either side of the blastodisc apex. During a second assembly and extension phase, F-actin patches accumulate at, and fuse to, the growing ends of the initial arc, resulting in its extension to the edge of the blastodisc. We propose that this represents a biphasic mode of assembly and extension of the contractile apparatus during the first few cell division cycles in zebrafish embryos, and that this strategy is a consequence of the large size of these cells. MLC2 does not appear to be recruited to the initial F-actin arc. However, clusters of MLC2 are recruited to, and incorporated into, the growing ends of the contractile band. We suggest, therefore, that the initial MLC2-free arc serves to position the furrow in the correct cleavage plane, and provides a scaffold for further assembly and extension of the contractile apparatus across the blastodisc. The main contractile force, therefore, is generated by the lateral ends of the contractile apparatus where MLC2 is incorporated. A schematic outlining our proposed biphasic assembly of the contractile apparatus during the first meroblastic division of the zebrafish blastodisc is shown in Fig. 3. Finally, we suggest that in zebrafish, as has been previously reported from *Xenopus* and fission yeast, some form of interaction between F-actin and myosin II is required to assemble and extend the contractile apparatus.

Acknowledgements

We acknowledge financial support from the Hong Kong Research Grants Council GRF awards:

HKUST662109 and 662211; from the Hong Kong University Grants Committee (HK UGC) award: SEG_HKUST01, the HK UGC Theme Based Research Scheme award: T13–706/11–1, and from the Royal Society International Joint Project Award 2010/R1.

References

Agassiz, A. & Whitman, C. O. (1884). XIV. On the development of some pelagic fish eggs–preliminary notice. *Proc. Amer. Acad. Arts Sci.* **20**, 23–55.

Chang, D. C. & Meng, C., (1995). A localized elevation of cytosolic free calcium is associated with cytokinesis in the zebrafish embryo. *J. Cell Biol.* **131**, 1539–45.

Denis-Donini, S., Baccetti, B. & Monroy, A. (1976). Morphological changes of the surface of the eggs of *Xenopus laevis* in the course of development. 2. Cytokinesis and early cleavage. *J. Ult. Res.* **57**, 104–12.

Fluck, R. A., Miller, A. L. & Jaffe, L. A. (1991). Slow calcium waves accompany cytokinesis in medaka fish eggs. *J. Cell Biol.* **115**, 1259–65.

Fuentes, R. & Fernández, J. (2010). Ooplasmic segregation in the zebrafish zygote and early embryo: Pattern of ooplasmic movements and transport pathways. *Dev. Dyn.* **239**, 2172–89.

Gonda, K., Katoh, M., Hanyu, K., Watanabe, Y. & Numata, O. (1999). Ca^{2+}/calmodulin and p85 cooperatively regulate an initiation of cytokinesis in *Tetrahymena*. *J. Cell Sci.* **112**, 3619–26.

Kamito, A. (1928). Early development of the Japanese killifish (*Oryzias latipes*), with notes on its habits. *J. Coll. Agr. Univ. Tokyo.* **10**, 21–38.

Kimmel, C. B. & Law, R. D. (1985). Cell lineage of zebrafish blastomeres. I. Cleavage pattern and cytoplasmic bridges between cells. *Dev. Biol.* **108**, 78–85.

Kimmel, C. B., Ballard, W. W., Kimmel, S. R., Ullmann, B. & Schilling, T. F. (1995). Stages of embryonic development of the zebrafish. *Dev. Dyn.* **203**, 253–310.

Kishimoto, Y., Koshida, S., Furutani-Seiki, M. & Kondoh, H. (2004). Zebrafish maternal-effect mutations causing cytokinesis defect without affecting mitosis or equatorial *vasa* deposition. *Mech. Dev.* **121**, 79–89.

Lee, K. W., Webb, S. E. & Miller, A. L. (2003). Ca^{2+} released via IP_3 receptors is required for furrow deepening during cytokinesis in zebrafish eggs. *Int. J. Dev. Biol.* **47**, 411–21.

Lee, K. W., Ho, S. M., Wong, C. H., Webb, S. E. & Miller, A. L. (2004).Characterization of mid-spindle microtubules during furrow positioning in early cleavage period zebrafish embryos. *Zygote* **12**, 221–30.

Lee, K. W., Webb, S. E. & Miller, A. L. (2006). Requirement for a localized, IP_3R-generated Ca^{2+} transient during the furrow positioning process in zebrafish zygotes. *Zygote* **14**, 143–55.

Lentz, T. L. & Trinkaus, J. P. (1967). A fine structural study of cytodifferentiation during cleavage, blastula, and gastrula stages of *Fundulus heteroclitus*. *J. Cell Biol.* **32**, 121–38.

Leung, C. F., Webb, S. E. & Miller, A. L. (1998). Calcium transients accompany ooplasmic segregation in zebrafish embryos. *Dev. Growth Differ.* **40**, 313–26.

Li, C-J., Heim, R., Lu, P., Pu, Y., Tsien, R. Y. & Chang, D. C. (1999). Dynamic redistribution of calmodulin in HeLa cells during cell division as revealed by a GFP-calmodulin fusion protein technique. *J. Cell Sci.* **112**, 1567–77.

Li, W. M., Webb, S. E., Chan, C. M. & Miller, A. L. (2008). Multiple roles of the furrow deepening Ca^{2+} transient during cytokinesis in zebrafish. *Dev. Biol.* **316**, 228–48.

Mabuchi, I. (1994). Cleavage furrow: timing and emergence of contractile ring actin filaments and establishment of the contractile ring by filament bundling in sea urchin eggs. *J. Cell Sci.* **107**, 1853–62.

Matsumura, F. (2005). Regulation of myosin II during cytokinesis in higher eukaryotes. *Trends Cell Biol*. **15**, 371–7.

Motegi, F., Nakano, K. & Mabuchi, I. (2000). Molecular mechanisms of myosin-II assembly at the division site in *Schizosaccharomyces pombe*. *J. Cell Sci.* **113**, 1813–25.

Naqvi, N. I., Eng, K., Gould, K. L. & Balasubramanian, M. K. (1999). Evidence for F-actin-dependent and–independent mechanisms involved in assembly and stability of the medial actomyosin ring in fission yeast. *EMBO J.* **15**, 854–62.

Noguchi, T. & Mabuchi, I. (2001). Reorganization of actin cytoskeleton at the growing end of the cleavage furrow of *Xenopus* egg during cytokinesis. *J. Cell Sci.* **114**, 401–12.

Rappaport, R. (1996). *Cytokinesis in Animal Cells*. Cambridge University Press, Cambridge, UK.

Satterwhite, L. L., Lohka, M. J., Wilson, K. L., Scherson, T. Y., Cisek, L. J., Corden, J. L. & Pollard, T. D. (1992). Phosphorylation of myosin II regulatory light chain by cyclin-p34cdc2: A mechanism for the timing of cytokinesis. *J. Cell Biol.* **118**, 596–605.

Schroeder, T. E. (1975). Dynamics of the contractile ring. In *Molecules and Cell Movement*, (eds S. Inoué & R. E. Stephens), pp. 305–34, Raven Press: New York.

Selman, G. C. & Perry, M. M. (1970). Ultrastructural changes in the surface layers of the newt's egg in relation to the mechanism of its cleavage. *J. Cell Sci.* **6**, 207–27.

Stone, V. J., Webb, T. A. & Fluck, R. A. (1993). Blastodisc morphology during first cleavage of the *Oryzias latipes* (medaka) fish egg. *The Fish Biol. J MEDAKA* **5**, 17–21.

Takayama, M., Noguchi, T., Yamashiro, S. & Mabuchi, I. (2002). Microtubule organization in *Xenopus* eggs during the first cleavage and its role in cytokinesis. *Cell Struct. Funct.* **27**, 163–71.

Uehara, R., Goshima, G., Mabuchi, I., Vale, R. D., Spudich, J. A. & Griffis, E. R. (2010). Determinants of myosin II cortical localization during cytokinesis. *Curr. Biol.* **20**, 1080–5.

Urven, L. E., Yabe, T. & Pelegri, F. (2006). A role for non-muscle myosin II function in furrow maturation in the early zebrafish embryo. *J. Cell Sci.* **119**, 4342–52.

Webb, S. E., Lee, K. W., Karplus, E. & Miller, A. L. (1997). Localized calcium transients accompany furrow positioning, propagation, and deepening during the early cleavage period of zebrafish embryos. *Dev. Biol.* **192**, 78–92.

Webb, S. E., Fluck, R. A. & Miller, A. L. (2011). Calcium signaling during the early development of medaka and zebrafish. *Biochimie* **93**, 2112–25.

Westerfield, M. (1994). *The Zebrafish Book: A Guide for the Laboratory Use of Zebrafish* (Brachydanio rerio). Univ. of Oregon Press, Eugene, OR, USA.

Wilson, H. V. (1889). The embryology of the sea bass (*Serranus atarius*). *Bull. U.S. Fish Comm.* **9**, 209–77.

Yumura, S., Ueda, M., Sako, Y., Kitanishi-Yumura, T. & Yanagida, T. (2008). Multiple mechanisms for accumulation of myosin II filaments at the equator during cytokinesis. *Traffic* **9**, 2089–99.